



# Hydrochemical characterization and geospatial analysis of groundwater quality in Cap Bon region, northeastern Tunisia

Abdelaziz Sebei<sup>1</sup> · Tarek Slama<sup>1</sup> · Mohamed Amine Helali<sup>1</sup>

Received: 10 March 2018 / Accepted: 7 July 2018 / Published online: 1 August 2018  
© Springer-Verlag GmbH Germany, part of Springer Nature 2018

## Abstract

The hydrogeochemical characteristics of shallow groundwater in the Grombalia region, northeastern Tunisia, were investigated to evaluate suitability for irrigation and other uses and to determine the main processes that control its chemical composition. A total of 21 groundwater samples were collected from existing wells in January–February 2015 and were analyzed for the major cations and anions concentrations. Conductivity, pH,  $T^{\circ}$ ,  $O_2$  and salinity were also measured. Interrelationships between chemical parameters were determined by using the scatter matrix method. The suitability of groundwater for irrigation and other uses was assessed by determining the sodium adsorption ratio, soluble-sodium percentage, total dissolved solids, total hardness, Kelly's index and permeability index values of water samples. The spatial distribution of key parameters was assessed using a GIS-based spatial gridding technique. This analysis indicated that the chemical composition of groundwater in the study area is of Cl–SO<sub>4</sub>–Na–Ca mixed facies with concentrations of many chemical constituents exceeding known guideline values for irrigation. The salinity of groundwater is controlled by most dominant cation and anion (Na–Cl). A correlation analysis shows that Na<sup>+</sup> is the dominant cation and that reverse ion exchange is a dominant process that controls the hydrogeochemical evolution of groundwater in the area. Geospatial mapping of hydrochemical parameters and indices analyzed with the USSS and Wilcox diagrams show distinctive areas of irrigation suitability. In contrast, 76.2% of samples fall in the highly doubtful to unsuitable category and indicate that the central and north-eastern parts of the study area are unsuitable for irrigation due to a high salinity and alkalinity.

**Keywords** Hydrochemistry · Scatter matrix analysis · Geospatial zoning · Water quality · Grombalia aquifer

## Introduction

In arid and semi-arid areas, groundwater is often the dominant resource used for agricultural and industrial water supplies. During recent decades, it has been observed that the over-pumping and increasing land use activities are posing great threat to the availability of groundwater and to its quality all over the world (Mor et al. 2006).

These issues have also been reported in the Cap Bon, an agricultural area with various industrial activities in north-eastern Tunisia (Fig. 1). Large volumes of groundwater in this region are pumped from the Grombalia basin (GB) for agricultural, industrial and domestic purposes. The increased industrial and agricultural development of this region has also greatly increased the demand for water which has adversely affected the quality of both surface and groundwater resources in the region (Ben Moussa et al. 2009; Bouksila et al. 2013; Ameer et al. 2016). Moreover, with the absence of a management plan and significant groundwater management policies, groundwater use in some parts of the basin exceeds natural recharge rates (DGRE 1998; Sebei et al. 2004).

In addition, the GB aquifer is considered to be the most vulnerable aquifer in the region since it is a shallow near-coastal aquifers system that is highly vulnerable to contamination. These conditions impose significant management challenges and there is a need for rigorous policies to protect

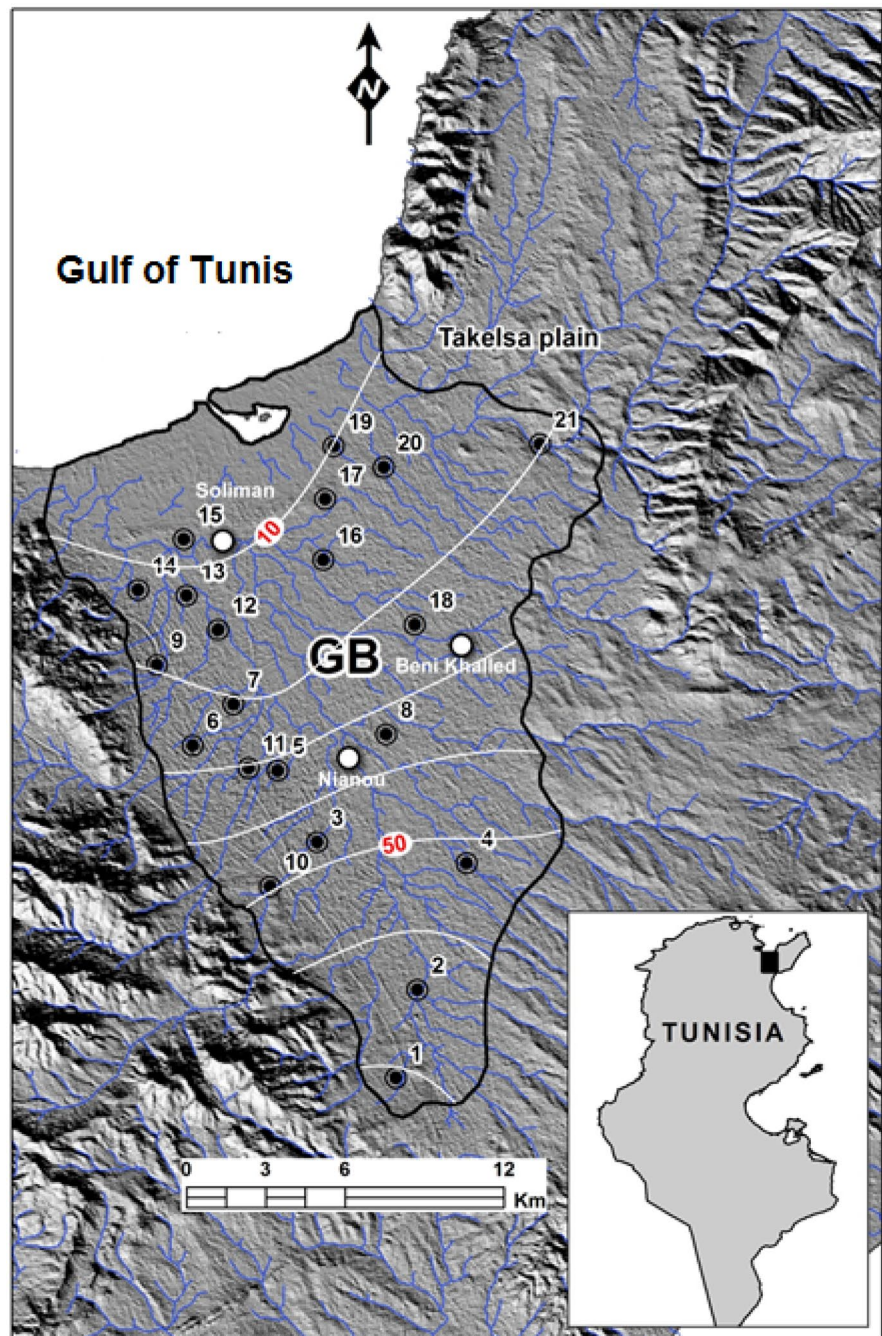
✉ Abdelaziz Sebei  
abdelaziz.sebei@fst.utm.tn

Tarek Slama  
trslama@gmail.com

Mohamed Amine Helali  
he.amine@gmail.com

<sup>1</sup> Faculty of Sciences of Tunis, Department of Geology, University of Tunis El Manar, El Manar II, 2092 Tunis, Tunisia

**Fig. 1** Location map of Grombalia basin (GB) with water wells emplacements and contours of the piezometric map (white lines, Tlili-Zrelli 2013, modified)



groundwater quality and to manage groundwater availability in this region.

Some anthropogenic and natural sources of contamination of the groundwater resources in the GB aquifer have been highlighted recently. It seems that the salinization problem highlighted within this aquifer results especially from seawater intrusion. However, chemical pollution has also been caused by agricultural and industrial activities in the region (Trabelsi et al. 2013).

The groundwater resources in the GB are highly vulnerable to groundwater contamination from existing land uses

in the region. Consequently, ongoing groundwater monitoring will be required in the region to assess land use impacts on water quality and to determine the chemical processes that control the natural evolution of groundwater quality in the shallow aquifer.

Water quality analysis, which is primarily based on hydrochemical investigations, is one of the most important methods used for assessing the chemical characteristics of groundwater resources. It involves various multidisciplinary approaches to assessing groundwater quality using geochemical associations and ratios and statistical

and graphical approaches (e.g., Kim et al. 2002; Salem et al. 2015; Tziritis et al. 2016). Among the graphical method, the mapping of spatial variability of major ion concentrations is a useful tool that enables the synoptic spatial distribution to be determined of chemical elements that control groundwater quality.

The concern of groundwater salinization has been discussed in many regions in the world under various geological and environmental conditions using several geochemical and statistical approaches. Groundwater salinization may occur from different sources and hydrogeochemical processes that control groundwater geochemistry as much as the infiltration of wastewater, irrigation returns, dissolution of evaporitic rocks and sea water intrusion (Custodio 1993; Kim et al. 2003; Wang and Jiao 2012). Hydrochemical and isotopic geochemistry and others standard methods based on the analysis of the relationships of major elements and environmental isotopes in groundwater are acknowledged as conventional approaches to investigate the origin and the evolution of groundwater salinization (e.g., Bennetts et al. 2006; Carol et al. 2009; Chen et al. 2013; Gil-Márquez et al. 2017; Liu et al. 2016; Argamasilla et al. 2017). In many complex case studies where many hydrochemical factors and processes involved in the aquifer system, conventional methods are unable to identify the driving factors controlling the groundwater chemistry. However, multivariate statistical analyses are conversely applied in processing and interpreting geochemical data because of their ability to simplify the complex interrelationships of many factors and to reveal interactions and correlations between diverse variables (Mohapatra et al. 2011; Okiongbo and Douglas 2015; Tziritis et al. 2016; Thivya et al. 2017). Several multivariate statistical approaches have been used (and sometime customized) for complex case study as much as coastal aquifer systems where salinization occurs mainly from sea water intrusion (e.g., Petalas and Lambrakis 2006; Papatheodorou et al. 2007; Arslan 2013; Abu-alnaeem et al. 2018; Boughariou et al. 2018; Ntanganedzeni et al. 2018).

In this paper, a hydrochemical study of the coastal aquifer system in Grombalia basin, northeastern Tunisia has been carried out on 21 groundwater samples collected in 2015, using statistical procedures and geospatial mapping techniques. This study aims to determine the geochemical characteristics of groundwater resources in this aquifer to enable a better understanding of the processes that affect groundwater quality in the region. The evaluation of the groundwater quality and the delineation of sensitive and high-risk areas are also made.

## Study area

### General settings

The GB is located in the western part of the Cap Bon peninsula in Tunisia and to the south of the Gulf of Tunis (Fig. 1). It constitutes a coastal plain with an area of ~364 km<sup>2</sup>. Since the soils within this plain are mostly fertile, lands devoted to agriculture occupies the largest part of the GB, even at the coast. The plain is located within semi-arid and sub-humid climatic zones. The average annual temperature is about 18 °C and the potential evapotranspiration (PE or ETP) is around 1300 mm/year (Arnould and Hotyat 2003). The annual rainfall ranges between 450 and 550 mm and mostly takes place during the relatively mild winter months. The average elevation of land overlying the basis is about 39 m. The basin is bordered to the west by the highlands of Jebel el Mokta, Jebel Halloufa and Jebel Bou Choucha that are up to about 700 m in elevation, and to the east, it is bordered by Jebel Abderrahmen (Fig. 2b). Rainfall over highlands to the west of the GB is significant source of runoff that is discharged to the plain. The landscape is shaped by a well-developed drainage network with some streams connected to the main wadis of Belli, El Melah, Bezirk, Bou Argoub, Soltan and El Bey (Fig. 2a). The lagoon system of Sebkhet el Melah (SEM) located to the northern part of GB is regarded as a distinct salt flats. Moreover, the structure and texture of soil layers are found to be modified with a high level of degradation in this area (Ben Moussa et al. 2009).

### Geology and hydrogeology

The study area is located in the northeastern extension of the Atlas fold belt of Tunisia to the southeast of the Tellian–Sicilian imbricate zone. This domain exhibits complex structural background that has chiefly controlled the deposition since Mesozoic times (Ben Ayed 1993; Bedir et al. 1996; Melki et al. 2010; Dhraief et al. 2017). The GB is an alluvial plain filled by Oligocene–Quaternary series mainly made of detrital and siliciclastic sediments eroded and transported to the area by an alluvial depositional system acknowledged at northeastern Tunisia scale for the Neogene–Quaternary times (Burolet 1956; Ben Ismail-Lattrache and Bobier 1984; Biely et al. 1972). This sedimentary sequence exhibits locally some intercalations of mudstones, clays and gypsum levels.

At the Cap Bon peninsula scale, the Oligocene–Early Miocene series comprise the Fortuna Formation, a siliciclastic sequence made of siltstones, mudstones and sandstones that rest unconformably on Eocene sediments. This formation is overlaid by a sequence of sands, clays, gypsum and carbonates Langhian–Messinian in age which is called the

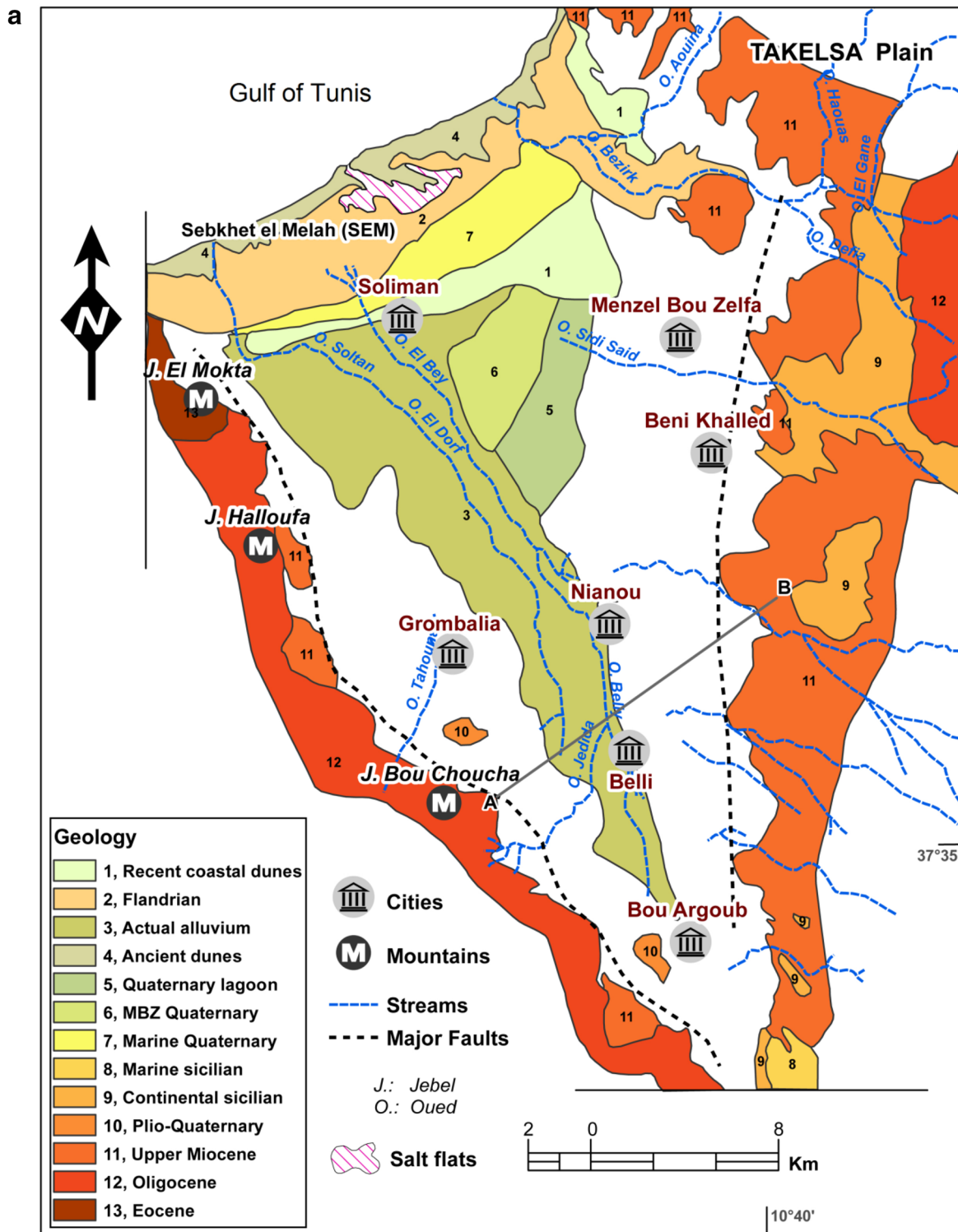


**Fig. 2 a, b** Geological map of Grombalia basin (Arnould 1950; Bujalka et al. 1971, modified). AB: cross section detailed below (Ennabli 1980, modified). MBZ Menzel Bou Zelfa

Oum Douil Group (Biely et al. 1972; Dhraief et al. 2017). In the GB, sediments of Oligocene age are represented by a 150-m-thick sandy sequence. This sequence is overlaid by

the Saouef Formation which is Middle Miocene in age and made of a sequence of sandstones and clays (Ben Salem 1992). Locally, near the southwest border of the GB, the

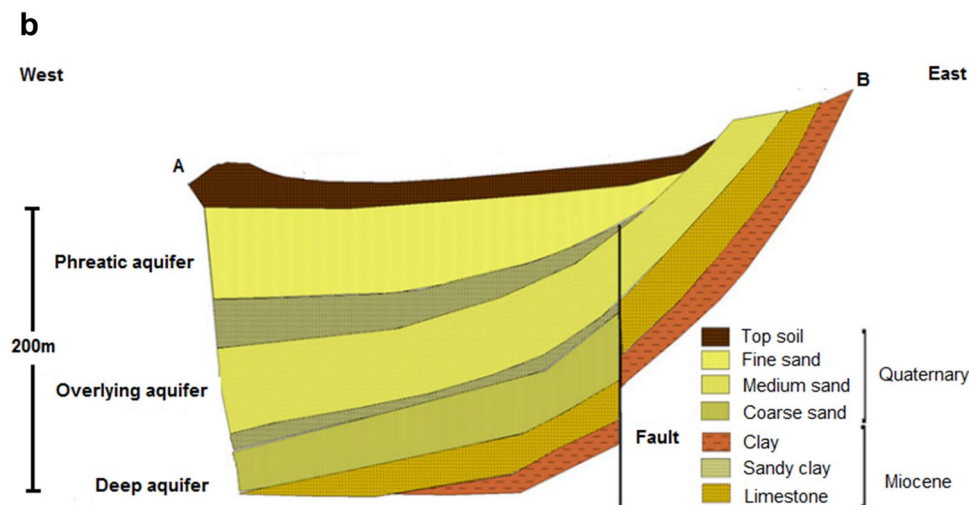


Fig. 2 (continued)

Miocene sediments mainly consist of marls with interbedded limestone members (Fig. 2a, b). The Pliocene series are composed of ~20-m-thick sandy sequence.

The GB consists of an asymmetric graben bordered by normal faults that were reactivated during the Middle Miocene (Chihi 1995; Hadj Sassi et al. 2006). This led to the establishment of a depositional area for the accumulation of post-Miocene sediments (Castany 1948). Consequently, this graben has been filled by a relatively thick continental Quaternary sequence comprising sands, marls and sandstones with intercalations of lagunal sandy layers (Chakroun et al. 2009) and a gypsum level at 130 m depth (Chihi 1995). The cross section of Fig. 2b shows a vertical throw of ~50 m along the N–S oriented normal fault that border the graben to the east; this throw collapsed the western bloc and led to the subsidence of the Quaternary series of sediments.

Overall the Quaternary fill of the graben consists of a sequence of detrital and porous materials with a high capacity to store and transmit groundwater. At the GB scale, these sediments form a shallow hydrogeological system with a thickness of about 350 m. However, based on the vertical variation of lithological units, this system is described as a multilayer aquifer with three distinctive aquifers which are (from top to bottom): (1) an unconfined phreatic aquifer within the uppermost Quaternary fine sand with an average thick of about 40 m (Ennabli 1980), but it can reach more than 100 m thick in the central part of the graben; (2) an overlying aquifer encased within the Quaternary medium sands and (3) a relatively deep aquifer within the Quaternary coarse sands and separated from the overlying aquifer by a sandy clay level. This aquifer extends to a depth of approximately 200 m in the central part of the graben (Fig. 2b).

The recharge of this aquifer system is by rainfall over the very porous and permeable detrital material of the phreatic

aquifer, and by the infiltration of surface runoff sourced from outside of the basin. Then the water that infiltrates through the phreatic aquifer flows gravitationally downward to the other levels of the aquifer system.

The piezometric map (Fig. 1) shows that the hydrostatic level of the aquifer decreases significantly toward the sea (Sebei et al. 2004). Additionally, the piezometric level of the GB aquifer has been lowered by up to 10 m during the dry years (Ennabli 1980; Ben Moussa et al. 2009). The main groundwater flow direction is roughly SE–NW with other directions being only of minor importance.

The hydraulic conductivity and horizontal transmissivity values (values between  $25 \times 10^{-4}$  and  $-2 \times 10^{-2}$  m<sup>2</sup>/s) of the phreatic aquifer vary greatly depending on the lithology of the aquifer sediments and could be correlated with the local increase of clay sediments (Ben Moussa et al. 2009).

## Materials and methods

### Sampling and analysis

Twenty-one groundwater samples were collected from available water supply wells that abstract water from the upper 40 m depth of the phreatic aquifer in the GB during January–February 2015 (Fig. 1). During sampling, the basic field methods and precautions were taken. Each sample was carefully sealed, labeled, and taken to the laboratory for chemical analysis. Physicochemical parameters [pH, electrical conductivity (EC), dissolved oxygen, water salinity and temperature] were measured using digital WTW pH and conductivity meters (Table 1). Chemical analysis of cation elements (Ca<sup>2+</sup>, Mg<sup>2+</sup>, Na<sup>+</sup>, K<sup>+</sup>) were performed by spectrometric analysis using an atomic absorption spectrometer.

**Table 1** Physicochemical analyses of sampled data (January–February 2015) of GB aquifer

Sample	<i>T</i> (°C)	pH	O <sub>2</sub> (mg/l)	Salinity (g/l)	E.C (ms/cm)	Na <sup>+</sup>	K <sup>+</sup>	Mg <sup>2+</sup>	Ca <sup>2+</sup>	SO <sub>4</sub> <sup>2-</sup>	Cl <sup>-</sup>	HCO <sub>3</sub> <sup>-</sup>
1	18.8	7.84	5.8	1	1.78	283.13	12.09	53.28	197	528	426	183
2	19.5	7.46	6.6	2.3	3.88	387.32	34.71	138.24	364.2	552	1029.5	305
3	19.2	7.38	4.9	2.3	3.89	406.64	6.63	100.68	308	696.96	781	244
4	18.7	7.47	6.7	2.2	3.64	396.75	13.65	114.72	274.8	537.6	958.5	231.8
5	19.6	7.05	5.7	2.1	3.58	272.55	9.75	104.88	264.2	376.32	816.5	195.2
6	18.5	7.15	5.7	1.1	1.88	232.76	10.14	42.72	144.2	490.08	195.25	244
7	19.2	7.27	4.3	1.2	1.92	316.25	12.09	61.44	164.6	686.4	390.5	122
8	18.5	7.37	5.8	2.8	4.51	764.75	5.46	124.08	349	778.08	1562	170.8
9	17.3	7.03	6.5	1.1	1.88	181.47	11.7	49.44	145.2	398.4	319.5	115.9
10	20.2	7.2	4.8	0.9	1.71	165.83	10.92	46.08	119.4	329.76	319.5	122
11	18.4	7.11	6.7	1.3	2.54	280.6	6.63	74.04	217.8	384	639	164.7
12	18.7	7.09	4.1	2.7	4.21	695.75	5.85	122.52	364.2	1056	1136	280.6
13	19.5	7.1	6.8	1.2	2.22	212.52	5.46	68.88	157	408	461.5	128.1
14	18.9	7.6	7.1	1.3	2.54	293.48	6.63	70.08	224	346.08	603.5	231.8
15	19.2	7.43	7.5	4	6.32	1150	15.21	194.52	506	1488	2059	311.1
14	17.2	7.15	6.7	2.8	4.51	856.75	38.22	121.92	396	1296	1260.25	256.2
17	18.2	7.13	5.9	4.2	6.87	1063.75	15.21	185.28	485.2	1248	1917	298.9
18	20.2	7.89	5.7	2.1	3.54	342.01	14.43	64.8	337.8	528	887.5	146.4
19	19.4	7.33	7.2	3.6	5.01	830.76	23.01	152.88	424.2	1488	1313.5	231.8
20	18.9	7.29	6.1	2.4	4.21	401.35	10.53	84.252	330	528	887.5	189.1
21	17.8	7.21	7.2	1.3	2.37	180.32	8.19	38.52	209	432	390.5	128.1

Major ions values are in mg/l

Anion concentrations were estimated using standard analytical methods. All water quality parameters were analyzed based on common and standard methods intended for the examination of a variety of water qualities (APHA 1998).

Furthermore, ionic balances (IB error in Table 2) were undertaken on the chemical analyses for quality control purposes and the cation and anion ratio was computed for each sample (Freeze and Cherry 1979). Error values below  $\pm 5\%$  are the best analytical estimation and the accepted error level is no more than  $\pm 10\%$  (Danielsson et al. 1999; Andersen 2001). If the error percentage exceeds  $\pm 10\%$ , it means that there may be some errors (in calculations, or in the water sampling process). The IB error values of the studied samples varies between  $-6.34$  and  $2.13\%$  with an average value of  $-1.5\%$  (Table 2). 90.47% of our sample analyses have an IB error values less than  $\pm 5\%$ .

## Hydrogeochemistry

The suitability of groundwater quality for use is commonly assessed on the basis of a number of indices and parameters or attributes. Key parameters and calculated indices for studied samples are presented in Table 3.

TDS values were estimated using electrical conductivity measurements which is a good indicator of the total salinity within aquifer systems (Hiscock 2005). It can illustrate

groundwater quality and it is commonly used in understanding the effect of seawater intrusion (Khaki et al. 2015; Rusydi 2018). Harmful irrigation practices in coastal regions engender excessive pumping and overexploitation of groundwater which lead to long-term deterioration in groundwater quality especially by seawater intrusion and to chemical and structural degradation of soils. In such conditions, concentrations of sodium, calcium, magnesium and bicarbonate can be affected. The permeability index (PI) is thus expressed based on these ions (Table 3) and can be used to describe the soil/aquifer interaction (Raghunath 1987). Kelly's index is calculated by the concentrations in groundwater of sodium measured against calcium and magnesium and water samples are classified according to sodium excess or deficiency (Kelly 1951; Alam et al. 2012). Water samples are classified as suitable for irrigation if Kelly's index is below 1.

The total hardness (TH) which refers to the mineral content in a water sample is a function of calcium and magnesium concentrations (Table 3). Water is considered "soft" if TH is less than 75 ppm, "moderately hard" if TH is 75–150 ppm, "hard" if TH is 150–300 ppm, and "very hard" if TH exceed 300 ppm (Mosafieri et al. 2014). Seawater's hardness is typically in the range of 6630 ppm.

Sodium percent (%Na) or SSP is an important parameter to investigate the sodium diffusion hazard (alkali vulnerability). It is helpful in characterizing water hardness. High

**Table 2** Summary statistics of hydrochemical elements and parameters of GB aquifer

Parameters	N total	Min	Max	Mean	SD	Range	HWO <sup>a</sup>
Na <sup>+</sup> (mg/l)	21	165.83	1150.00	462.61	301.29	984.17	200
K <sup>+</sup> (mg/l)	21	5.46	38.22	13.17	8.84	32.76	30
Mg <sup>2+</sup> (mg/l)	21	38.52	194.52	95.87	45.90	156.00	150
Ca <sup>2+</sup> (mg/l)	21	119.40	506.00	284.85	114.58	386.60	200
SO <sub>4</sub> <sup>2-</sup> (mg/l)	21	329.76	1488.00	694.08	382.48	1158.24	400
Cl <sup>-</sup> (mg/l)	21	195.25	2059.00	873.98	522.61	1863.75	250
HCO <sub>3</sub> <sup>-</sup> (mg/l)	21	115.90	311.10	204.79	64.89	195.20	380
T (°C)	21	17.20	20.20	18.85	0.80	3.00	–
pH	21	7.03	7.89	7.31	0.24	0.86	6.5–8.5
O <sub>2</sub>	21	4.10	7.50	6.09	0.96	3.40	–
Salinity (g/l)	21	0.90	4.20	2.09	1.00	3.30	1.5
EC (ms/cm)	21	1.71	6.87	3.48	1.48	5.16	1.5
TDS (mg/l)	21	1113	5723	2629	1360	4610	1000
SAR (meq/l)	21	3.00	11.00	5.74	2.56	8.00	–
TH (ppm)	21	488	2064	1106	465	1576	500
SSP (%)	21	35.65	56.17	45.87	6.40	20.52	–
PI (%)	21	44.66	63.49	54.49	6.29	18.83	–
KI (meq/l)	21	0.54	1.25	0.86	0.23	0.71	–
IB error (%)	21	– 6.34	2.13	– 1.50	2.24	–	–

TH total hardness, SSP soluble-sodium percentage, PI permeability index, KI Kelly's index, IB ion balance  
<sup>a</sup>2011 data

**Table 3** Hydrochemical attributes and indices for irrigation suitability evaluation

Indices	Acronym	Formula	Adequate values	References
Sodium adsorption ratio	SAR (meq/l)	$\frac{Na^+}{\sqrt{\frac{Na^+ + Mg^{2+}}{2}}}$	< 10 meq/l	Richard (1954), Gupta et al. (2016)
Soluble-sodium percentage	%Na or SSP (meq/l)	$\frac{(Na^+ + K^+) \times 100}{(Ca^{2+} + Mg^{2+} + Na^+ + K^+)}$	< 60%	Wilcox (1955), Smith et al. (2015)
Total dissolved solids	TDS (mg/l)	ke EC (μS/cm)	< 2000 mg/l	Freeze and Cherry (1979)
Total hardness	TH (ppm)	2.497 Ca <sup>2+</sup> + 4.115 Mg <sup>2+</sup>	Between 100 and 150 ppm	WHO (2011)
Kelly's index	KI (meq/l)	$\frac{Na^+}{Ca^{2+} + Mg^{2+}}$	< 1 meq/l	Alam et al. (2012)
Permeability index	PI (ppm)	$\frac{Na^+ + \sqrt{HCO_3^-}}{Ca^{2+} + Mg^{2+} + Na^+} \times 100$	< 60%	Raghunath (1987)

values of %Na indicate a soft water and low values indicate hard water (Wilcox 1955). In fact, the increase of sodium in irrigation water possibly leads to Na<sup>+</sup> adsorption by clay particles and to Mg<sup>2+</sup> and Ca<sup>2+</sup> ions displacing. In addition, the sodium hazard of irrigation water can also be evaluated using the sodium adsorption ratio (SAR: Richards 1954). The magnitude of the soil sodicity hazard that is associated with SAR values can be classified as follows: “low” (SAR < 10), “medium” (SAR, 10–18), “high” (SAR, 18–26), and “very high” (SAR > 26).

Piper, USSL and Wilcox diagrams have been drawn using the results of chemical analyses of groundwater samples then interpreted to determine the water type and the different indices of water suitability for irrigation including salinity,

sodicity, and bicarbonate concentrations. Moreover, nine maps have been processed to determine the spatial distribution of the nine following attributes/indices; salinity, SAR, TH, pH, %Na, KI, EC, TDS and PI. This mapping was carried by automated processing and kriging of georeferenced hydrochemical data in a geographical information system. Obtained maps can be used for assessing water quality data to enable sound management decisions to be made (Mosafieri et al. 2014).

## Results and discussion

### Groundwater chemistry and main properties

The quality of groundwater was assessed by comparison with guidelines established for livestock and irrigation. The major characteristics to be considered for water used in agriculture are salinity and sodicity. Concentrations of major ions and related physicochemical parameters and attributes determined in this study are summarized in Table 2 together with key statistical attributes of the results.

The pH of analyzed water samples ranges between 7.03 and 7.89 with an average of 7.31, indicating a neutral to mildly alkaline groundwater in the GB aquifer. The pH of water plays an important role in various types of geochemical equilibrium. In fact, along with alkalinity it affects the solubility and availability of nutrients and other chemical characteristics of irrigation water.

Groundwater salinity ranges between from 0.9 to 4.20 g/l with an average value of 2.09 g/l and a standard deviation around 1. It indicates the amount of dissolved salts in water which generally comes from weathering of soil and sediments leaching. However, if the balance between groundwater abstraction and natural recharge is affected, seawater intrusion became an eminent source of groundwater salinization. The salinity varies seasonally because of the seasonality of precipitations and the evapotranspiration intensity (Bouksila et al. 2013); the amount of salt found in irrigation water is usually greater in arid and semi-arid areas. In fact salinity affects significantly the agricultural productivity by deteriorating soil properties and decreasing plant growth performance. It is worth noting that measured mean values of salinity and EC (about 3.48 mS/cm) in the GB aquifer exceed the World Health Organization (WHO) standards values for drinking water and for irrigation use (Table 2).

TDS mainly indicates the various kinds of minerals present in the water and typically is closely correlated with the conductivity levels in water (Hiscock 2005). TDS values of groundwater samples in the GB aquifer exceed the WHO standard values of 1000 mg/l; they vary from 1113 to 5723 mg/l with a mean value of 2629 mg/l.

TH values range from 488 to 2064 ppm with an average of 1106 ppm. These values (Table 2) indicate that groundwater of the GB aquifer is very hard. The hardness of water is due to the high concentrations of the alkaline earth elements, calcium and magnesium which are essential plant nutrients. Moderate levels of hardness in groundwater (100–150 ppm) are considered ideal for plant growth.

SAR is commonly used to assess the relative concentrations of  $\text{Na}^+$ ,  $\text{Ca}^{2+}$  and  $\text{Mg}^{2+}$  in irrigation water. It is

a helpful indicator of the potential damaging effect of irrigation water on soil structure and permeability. The level of sodicity or alkali hazard is thus deduced and described. A SAR value below 2 meq/l is considered very safe for plants, especially if the  $\text{Na}^+$  concentration is below 50 mg/l. SAR values of the studied groundwater samples vary from 3 to 11 meq/l with an average of about 5.5 meq/l. Mean values of SSP (45.87%), PI (54.49%) and KI (0.89 meq/l) indicate that the groundwater of the GB aquifer is suitable for irrigation purposes (Table 3). In contrast, maximum values exceed standard guidelines, particularly for PI and KI (Table 2).

Figure 3a, b and Table 2 show that among the determined elements and parameters, only the mean values of  $\text{K}^+$ ,  $\text{Mg}^{2+}$  and  $\text{HCO}_3^-$  are below the WHO permissible standards. The maximum values of these parameters exceed generally the WHO standard values except the  $\text{HCO}_3^-$  value (311 vs 380 mg/l). In contrast, the box chart of Fig. 3a indicates the average values of concentrations in mg/l of the following elements  $\text{Cl}^-$  (874),  $\text{SO}_4^{2-}$  (694),  $\text{Na}^+$  (463) and  $\text{Ca}^{2+}$  (265). All these values exceed these of the WHO guideline, particularly the  $\text{Cl}^-$ ,  $\text{SO}_4^{2-}$  and  $\text{Na}^+$  values (Fig. 3b). Chloride ( $\text{Cl}^-$ ) greatly exceeds the permissible limit of about 620 mg/l. The presence of high concentration of  $\text{Cl}^-$  in the GB aquifer suggests that there is a considerable anthropogenic contribution of this ion in groundwater, such as domestic wastewater and industrial discharges. Sodium ( $\text{Na}$ ) concentrations exceed 1100 mg/l locally and are most likely derived from the weathering of silicate and evaporitic rocks. Moreover, sodium displacement from the absorbed complex of rocks and soil by  $\text{Ca}^{2+}$  and  $\text{Mg}^{2+}$  could also contribute to water enrichment with  $\text{Na}^+$ . Generally, large concentrations of  $\text{Cl}^-$  and  $\text{Na}^+$  increase the corrosiveness of water and give water a salty taste. It is therefore suggested that  $\text{Na}^+$  and  $\text{Cl}^-$  ions may have the same origin, possibly related to the halite dissolution (Ben Moussa et al. 2009).

The  $\text{SO}_4^{2-}$  concentrations of analyzed water samples mostly exceed the guideline values. The main source of sulfate in these samples seems to be the dissolution of gypsum and anhydrite. However, the concentrations of  $\text{SO}_4^{2-}$  could be limited by the presence of  $\text{Ca}^{2+}$  ions (Gupta et al. 2016). In the GB aquifer, the highest values of sulphate ions concentration (~1450 mg/l) are observed within the samples 15, 16, 17 and 19 (Fig. 1) located at the southern margin of Sebkhel el Melah (SEM, Fig. 2). This could reveal the influence of the coastal sebkha system on the hydrochemistry of the GB groundwater.

$\text{Ca}^{2+}$  concentrations in the GB aquifer vary from 119 to 506 mg/l with an average of 285 mg/l. Slight calcium enrichment with concentrations of about 500 mg/l is observed in the coastal area around the SEM system. Alterations of limestone crust and gypsumiferous soils (calcium sulphate) by water



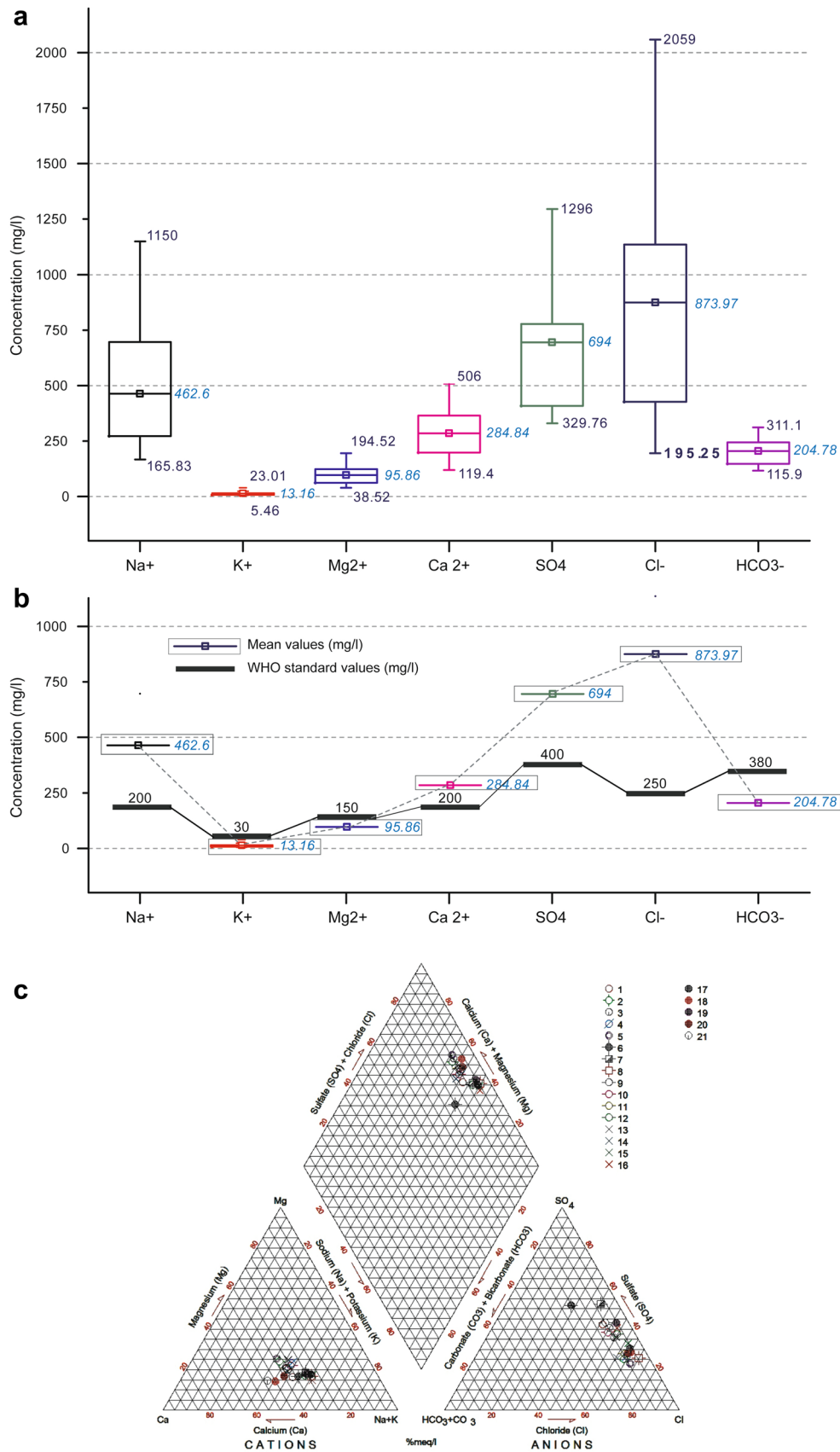


Fig. 3 Box chart of major ions (a) and comparison with WHO permissible values (b, 2011 data); Piper diagram showing hydrogeochemical facies of GB (c)

leakage into the aquifer in the northeastern part of the GB could explain these values.

The potassium content is an important parameter for water quality assessment.  $K^+$  concentrations in the analyzed water samples range from 5 to 38 mg/l and the mean value is 13.17 mg/l. The low level of  $K^+$  in natural waters is a consequence of its tendency to be fixed by clay minerals and to participate in the formation of secondary minerals. Levels above 10 mg/l may indicate water contamination from fertilizers or other anthropogenic sources. Consequently, increased potassium concentrations detected within the samples 2 and 16 (up to 38 mg/l) are indeed indicative of anthropogenic source close to these sites located, respectively, at the vicinity of the industrial zone of Bou Argoub and the industrial complex of Soliman (Figs. 1, 2a).

Magnesium concentrations of the analyzed groundwater samples range from 39 to 195 mg/l with an average value of 96 mg/l. The content of this ion within the GB aquifer is generally lower than that of calcium.

In general, concentrations of the major ions increase towards the coastal zone of the GB. This suggests that the SEM system and its surrounding saline soils together with seawater intrusion affect the groundwater quality toward the coast as mentioned by Sebei et al. (2004). Nevertheless, the chemistry of the studied aquifer seems to have a chemical composition dominated by the ions  $Cl-SO_4-Na-Ca$ . It is observed that chloride is the dominant anion which is supported by a graphical analysis and compositional classification by a Piper diagram (Fig. 3c).

### Hydrogeochemical facies

A Piper diagram was plotted to classify the hydrochemical water types based on the ionic composition of analyzed water samples. This classification can help in the interpretation of the geochemical facies, the hydrochemical conditions and related processes within the aquifer. The plotted Piper diagram (Fig. 3c) shows that the hydrochemical facies of groundwater in the GB is mainly of chloride type (Cl) mixed with sodium (Na), sulphate ( $SO_4$ ) and calcium (Ca) types, respectively, in the order of concentrations. The groundwater of the GB aquifer falls under  $Cl-Na-SO_4-Ca$  category and shows that chloride is the most dominant anion and sodium is the most dominant cation. Consequently, groundwater in the area is of  $Na-Cl$  type. However, this study reveals that the majority of groundwater samples fall in 'strong acids-exceed weak acids' group controlled mainly by  $(Cl+SO_4)$  which are the strong acid anions.

$HCO_3^-$ ,  $Mg^{2+}$  and  $K^+$  ions are relatively less represented in the groundwater of the GB. This groundwater depletion could be closely related to low sediment yield. In fact, magnesium in water (and so calcium and bicarbonate) tends to originate from the carbonate rocks (limestone) via natural

dissolution process (Taylor 1958). However,  $HCO_3^-$  can also be released from the reaction of feldspar minerals with carbonic acid in the presence of water (Elango et al. 2003).

### Groundwater hydrochemistry and salinization

#### Scatter matrix analysis of major ions

The interdependence and/or the correlations between all major ions were examined using the scatter matrix method (Fig. 4). In multivariate statistics, the scatter matrix is a statistical tool that is used to make an estimation of the covariance matrix (Davis 2002). It can be used to determine whether the variables are correlated and whether the correlation is positive or negative. Therefore, it is a graphical statistical representation for estimating the relationships among variables. Linear regression is mathematical model that was used to examine these relationships. The adjusted coefficient of determination  $R^2$  (Adj.  $R^2$ ) was employed to evaluate the level of linearity between variables as well as the efficiency of the prediction model. It ranges between 0 and 1 with a better fitting model for values close to 1. Also, the linear correlation ( $r$ ) between measured variables (major ions) and their interdependence was evaluated based on Pearson's  $r$  index. It varies between +1 and -1 and for positive and high correlation;  $X$  and  $Y$  variables are closely interdependent (Davis 2002).

The graphical plotting of scatter matrix and the estimation of assessment indices (Adj.  $R^2$  and Pearson's  $r$ ) were calculated with Origin Pro software (2015). The interpretation of this statistical analysis was carried out based on the level of correlation and the spatial dependence between studied major ions.

Considering each variable (or ion) on the  $X$  axis, the strength of linear relationships and the degree of ionic interdependence was analyzed and classified into four classes based on the number of involved ions (Fig. 4):

- Class I (with 4 ions):  $Na^+$  vs  $Cl^-$ ,  $SO_4^{2-}$ ,  $Ca^{2+}$ ,  $Mg^{2+}$  which is more significant for  $Cl^-$  and  $SO_4^{2-}$  (Adj.  $R^2 = \sim 0.88$  and Pearson's  $r = \sim 0.94$ );
- Class II (with 3 ions):  $Mg^{2+}$  vs  $Cl^-$ ,  $Ca^{2+}$  and  $Na^+$  which is more significant for  $Cl^-$  (Adj.  $R^2 = 0.89$  and Pearson's  $r = 0.94$ );  $Ca^{2+}$  vs  $Cl^-$ ,  $Mg^{2+}$  and  $Na^+$  which is more significant for  $Cl^-$  (Adj.  $R^2 = 0.89$  and Pearson's  $r = 0.94$ );  $Cl^-$  vs  $Ca^{2+}$ ,  $Mg^{2+}$  and  $Na^+$  which is more significant for  $Ca^{2+}$  and  $Mg^{2+}$  (Adj.  $R^2 = 0.89$  and Pearson's  $r = 0.94$ );
- Class III (with 1 ion):  $SO_4^{2-}$  vs  $Na^+$ ;
- Class IV (no reliable observations):  $K^+$  and  $HCO_3^-$  with low values of Adj.  $R^2$  and insignificant correlations.

On the basis of the graphical statistical representation, the relevant prediction model of distribution for major ions

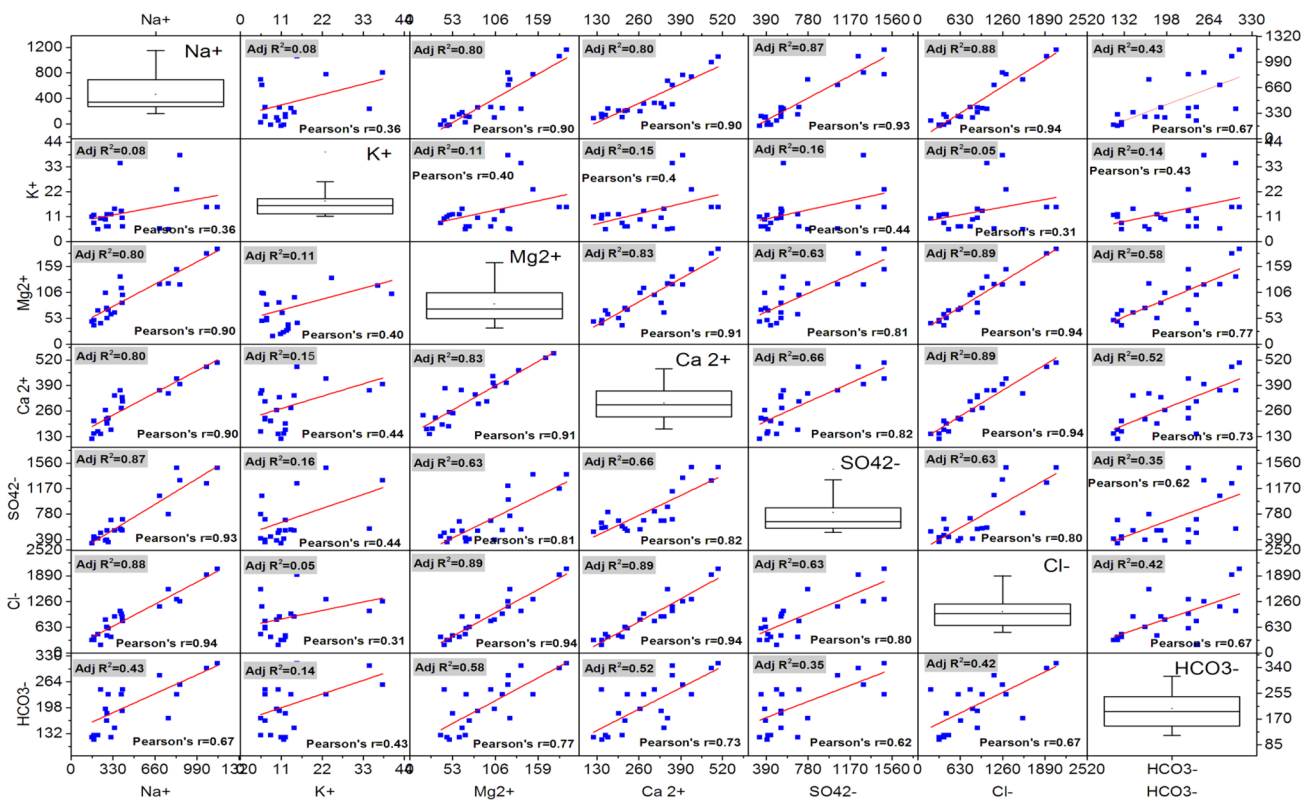


**Fig. 4** Scatter matrix diagram for major ions with statistical fitting/correlation analysis

with consistent correlation was well-defined for values close to 1. The classification of bivariate diagrams of the scatter matrix (Fig. 4) is considered for  $Adj. R^2 \geq 0.80$  and Pearson's  $r \geq 0.90$ . The class IV is considered for ions with relatively smallest values; thus  $K^+$  and  $HCO_3^-$  show no correlation with the other ions.  $Na^+$  is the most involved major ion in the hydrochemical processes of the GB aquifer; it defines the class I in association with  $Cl^-$ ,  $SO_4^{2-}$ ,  $Ca^{2+}$  and  $Mg^{2+}$ . It seems to come from silicates weathering which form the main fill of the GB and yields the studied groundwater samples. This is also deduced from hydrochemical facies which are controlled by  $Na^+$  and strong acid anions ( $Cl^- + SO_4$ ).

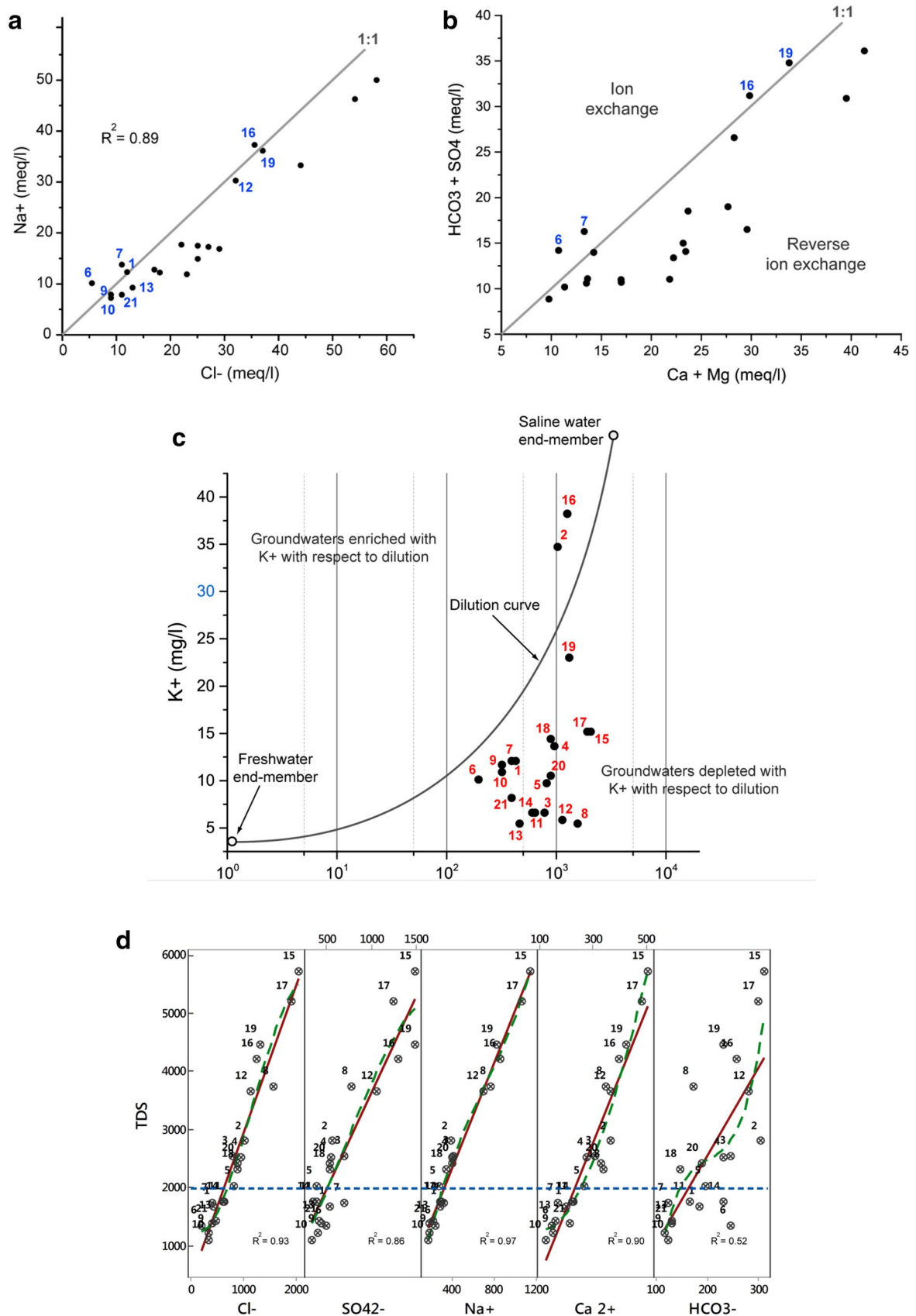
In class II, 3 major ions ( $Mg^{2+}$ ,  $Ca^{2+}$  and  $Cl^-$ ) are involved with more relevance for  $Cl^-$  despite its clear correlation with the two other ions. In the class III,  $SO_4^{2-}$  is significantly correlated with  $Na^+$  and has a coefficient value of 0.93. It seems that  $Na^+$  has influenced the spatial distribution of sulphate ( $SO_4^{2-}$ ) concentration as shown in Fig. 3a.

**Main hydrochemical processes**

Soluble constituents in groundwater come mainly from the dissolution of soils minerals in soils and sedimentary rocks. The amount of the various kinds of minerals present in the water defines the salinity and the chemical composition of

the groundwater which are relevant parameters for understanding the hydrochemical processes within the aquifer.

The bivariate plot in Fig. 5a indicates a high linear correlation between Na and Cl ( $R^2 = 0.89$ ); a common origin from halite dissolution in saline soils could explain this correlation. Plots with  $R^2$  above the line of 1:1 ratio are indicative of anion exchange process (Hiscock 2005) which concerns few groundwater samples (1, 6, and 7; Fig. 1) located within the piedplain area of the GB. Therefore, it seems that the Na-Cl reverse process prevails into the GB aquifer. The scatter diagram of ( $Ca^{2+} + Mg^{2+}$ ) vs ( $HCO_3^- + SO_4^{2-}$ ) in Fig. 5b shows that most of the samples deviate from the line of 1:1 ratio, which could indicate that sulphate reduction is taking place in the aquifer (Hiscock 2005). Also, groundwater mineralization and chemistry are mainly controlled by ion reverse exchange. In contrast, sulphate enrichment with ion exchange process is observed within the samples 6, 7, 16 and 19 (Figs. 1, 4b). In these locations, dissolution of calcite, dolomite, anhydrite, and gypsum seems to be the prevailing reactions. In fact, sulfate would have a common origin with Ca, but it has different geochemical behaviors with calcium especially in salt water. Moreover, the proportion of sodium in the adsorption complex is increased due to ion exchange processes. The development of gypsiferous soil layers is also observed (mainly in the SEM area, Fig. 2).



◀**Fig. 5** Graphical plots for exploring hydrochemical processes using scatter plots (a, b), the semi-logarithmic plot of a dilution diagram (c), and plots of TDS vs most influential ions (d)

The semi-logarithmic plot of dilution in the diagram of Fig. 5c shows a line that represents mixing between fresh and saline end-member groundwaters. Points plotting above and below the dilution curve represent, respectively, enrichment and depletion of the ionic concentration with respect to the conservative chloride ion. Figure 5c shows that groundwater  $K^+$  depletion concerns all samples except 2 and 16 which exhibit a particular  $K^+$  enrichment most likely due to an active anthropogenic/industrial source. For most samples,  $K^+$  concentration and distribution (Figs. 3a, b, 5c) are linked to over-irrigation, excessive fertilizer use and the discharge of domestic wastes.

### TDS analysis and groundwater salinization

The evaluation of groundwater total mineralization compared to ionic species is presented in Fig. 5d. We have considered most significant ions (Cl, Na,  $SO_4$  and Ca) and the less correlated one ( $HCO_3$ , Fig. 4). The plotted diagrams show a strong linear relationship for  $Cl^-$ ,  $Na^+$ ,  $SO_4^{2-}$  and  $Ca^{2+}$  with values close to 1. These positive correlations with TDS indicate that the referred elements contribute to the groundwater mineralization. In addition, sodium and chloride show the highest correlations with TDS (0.97 and 0.93, respectively) which indicates an obvious control of the groundwater salinity. A good correlation is also observed for  $SO_4^{2-}$  suggesting its participation with  $Na^+$  and  $Cl^-$  in water mineralization processes.

On the other hand, both bicarbonate and potassium ions show very poor correlations with TDS suggesting that these ions do not play an important role in the evolution of groundwater quality in the area.

### Water quality evaluation

#### Geospatial evolution of groundwater quality

In this study, nine hydrochemical parameters (salinity, SAR, TH, pH, %Na, KI, EC, TDS and PI) were gridded using GIS software to create corresponding geospatial distribution models (Fig. 6) presented as maps. These latter allow spatial analysis and geo-zoning of groundwater quality and permit to delimit suitable zones for irrigation purposes in the GB.

The GB aquifer has very hard water (TH > 300 mg/l as  $CaCO_3$ ) with values up to 2000 mg/l in the northern part of the area (Fig. 6). High concentrations of hardness may cause scaling contact surfaces, plug pipes and irrigation lines and can damage electrical appliances. They can also cause foliar scale deposits. Nevertheless, the removal of hardness by

using a water softener is necessary only if the water is causing problems. Referring to the WHO standards, the SAR, SSP (or %Na) and PI values (Table 3) of groundwaters sampled in the GB show that the aquifer is suitable for irrigation purposes except near the wells labeled 8, 15, 16 and 17. Samples 15, 16 and 17 are located to the north of the study area near the lagoon system of Sebkhet el Melah (Fig. 6). In this area SAR, SSP (or %Na) and PI values exceed largely WHO standards values and the groundwater are judged unsuitable for irrigation. High salinity, sodium enrichment (sodic hazard) and seawater leakage near the SEM system can explain this setting (Figs. 2a, 5d). However, sample 8 is located between two cities, Nianou and Beni Khalled, which implies anthropogenic sources.

TDS values in groundwater vary approximately from 1110 to 5700 mg/l. The lowest values (~1000 to 2000 mg/l) are mostly observed in the western part of the aquifer within the pediplain area of Jebel Halloufa and Bou Choucha/Bou Argoub (Fig. 2a). TDS above 2000 mg/l are very likely to cause plant growth problems. The lowest values of KI (~0.5 to 0.9 meq/l) and salinity (0.9–1.5 g/l) occupy approximately the same zone as TDS. This problem may occur when irrigation water contains relatively more sodium ions than divalent calcium and magnesium ions (KI). Accumulation of sodium ions can induce a breakdown of soil aggregates that are responsible for good soil structure needed for free movement of water and air through the soils.

Referring to the WHO standards and the spatial distribution hydrochemical parameters (Fig. 6), the western part of GB aquifer seems to have the most suitable water for safe irrigation. Furthermore, this area could be, in certain conditions, quite appropriate as a resource of drinking water (i.e., 3, 5, 9, 10, 11, 13, 14 and 21 wells). Due to the high values of hardness, less water treatments and adequate processing are occasionally needed.

### Classification of groundwater quality

The US salinity diagram (Fig. 7), which relates EC (a measure of the salinity hazard) and SAR (a measure of the alkalinity hazard), shows that the studied water samples are within C3, C4a and C4b categories. A total of 28.5% of the groundwater samples are of C3-S1 water type with high salinity and low sodium concentrations. This water may be used for irrigation in almost all types of soil with little danger of exchangeable sodium. In the western part of the GB, 61.9% of samples are classified into three categories: C4a-S1 (the most representative); C4a-S2; and C4a-S3. In this area water exhibits a very high salinity and a low alkalinity hazard and will be suitable for plants having a high tolerance to salts. Some localities into the pediplain area and the central part of GB are concerned (Fig. 6) as well as the Takelsa plain (sample 21, Fig. 1).

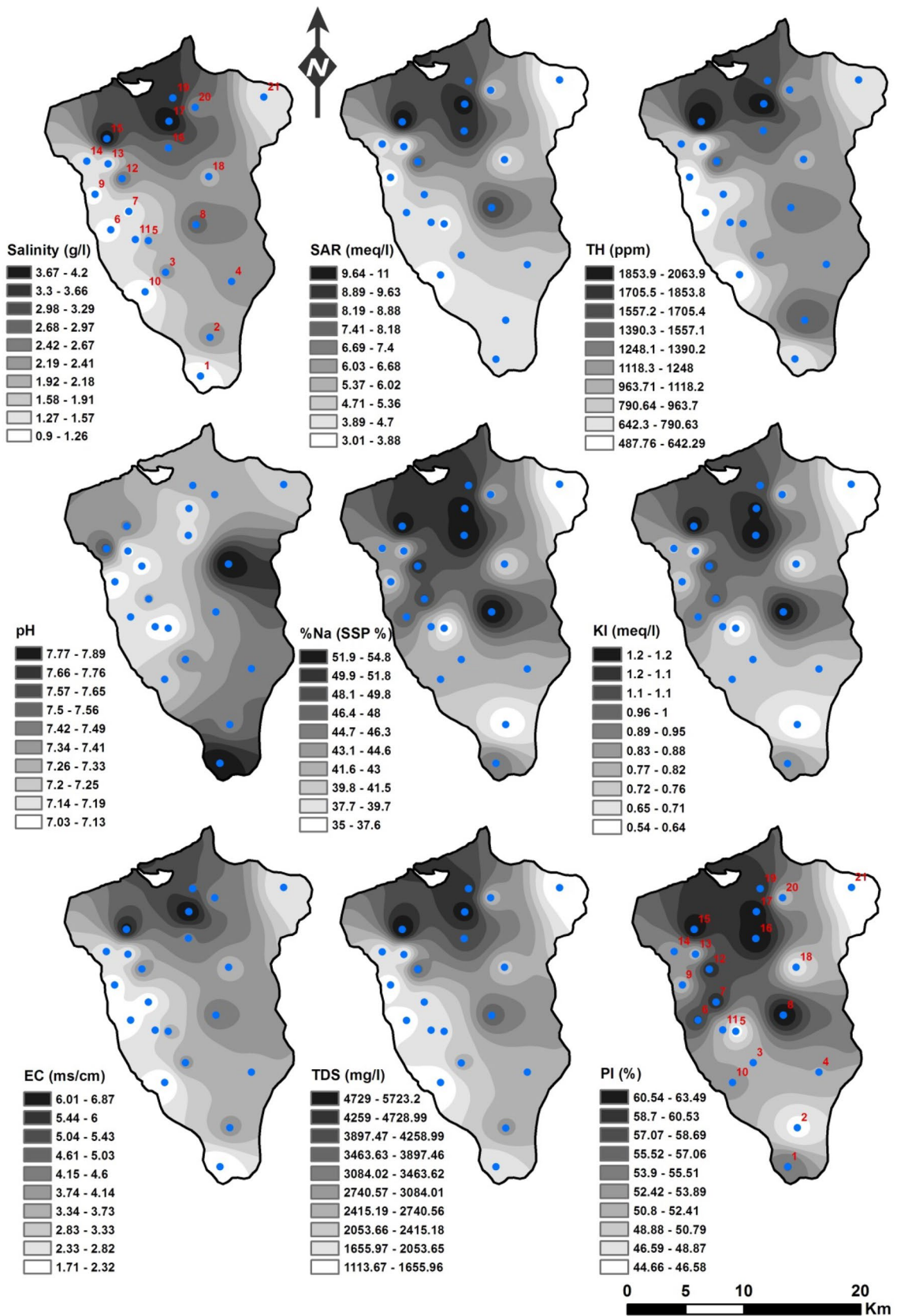


Fig. 6 Geospatial distribution of analyzed parameters and indices

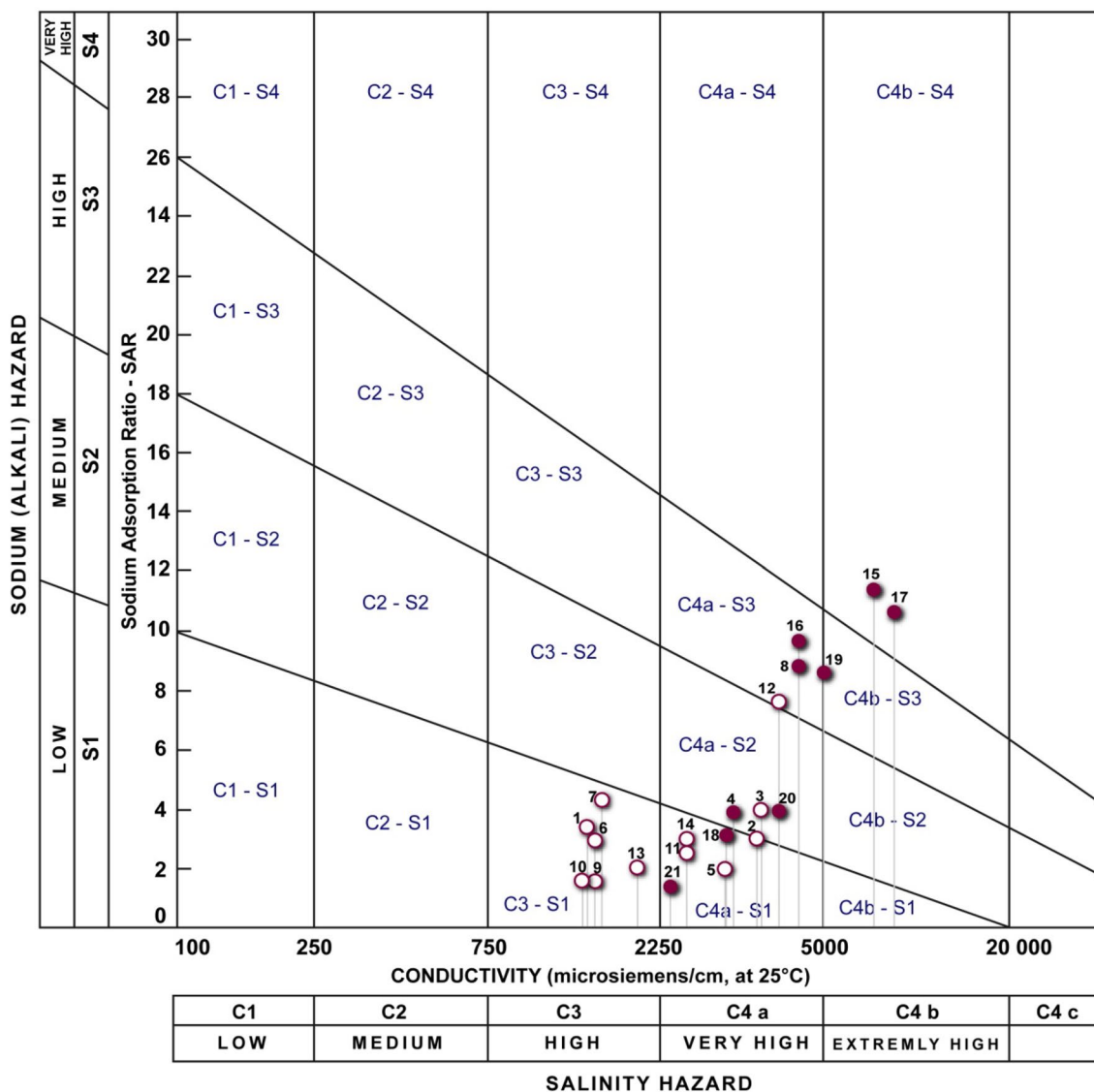


Fig. 7 USSS salinity hazard diagram for classification of water for irrigation. White-filled dots are located in the western part of GB

Samples 8, 12 and 16 are characterized by very high salinity and alkalinity hazards (C4a-S3) which indicates sodium enrichment with building-up of sodic soil layers.

The impact of the SEM system with seawater leakage is obviously evident for water samples 15, 17 and 19 (Fig. 7). They fall in the fields of C4b-S3 and S4 and exhibit an extremely high salinity and have a high alkalinity hazard. It is noticeable that there are no samples with low salinity and low alkalinity for the present case study which is also demonstrated with the spatial evolution of groundwater quality (Fig. 6).

Furthermore, a Wilcox diagram shows that some water samples (1, 6, 7, 9 and 10) are considered to be suitable for irrigation (Fig. 8) on the basis of both sodium percentage and EC (Wilcox 1955). About 24% of studies samples fall in this

category. They are located within the pediplain area of the GB aquifer. In the same region, 19% of samples are considered to be moderately suitable for irrigation. In contrast, 57% of samples have unsuitable irrigation quality, mostly those located in the central and northern areas of the GB. At the GB scale, it appears that the western margin of the pediplain (Fig. 1) is the most suitable area for adequate and safe irrigation with a groundwater potential estimated to 24%.

### Conclusions

An investigation involving the physicochemical analysis of groundwater samples, statistical procedures and geospatial mapping using GIS techniques in the GB highlighted that the

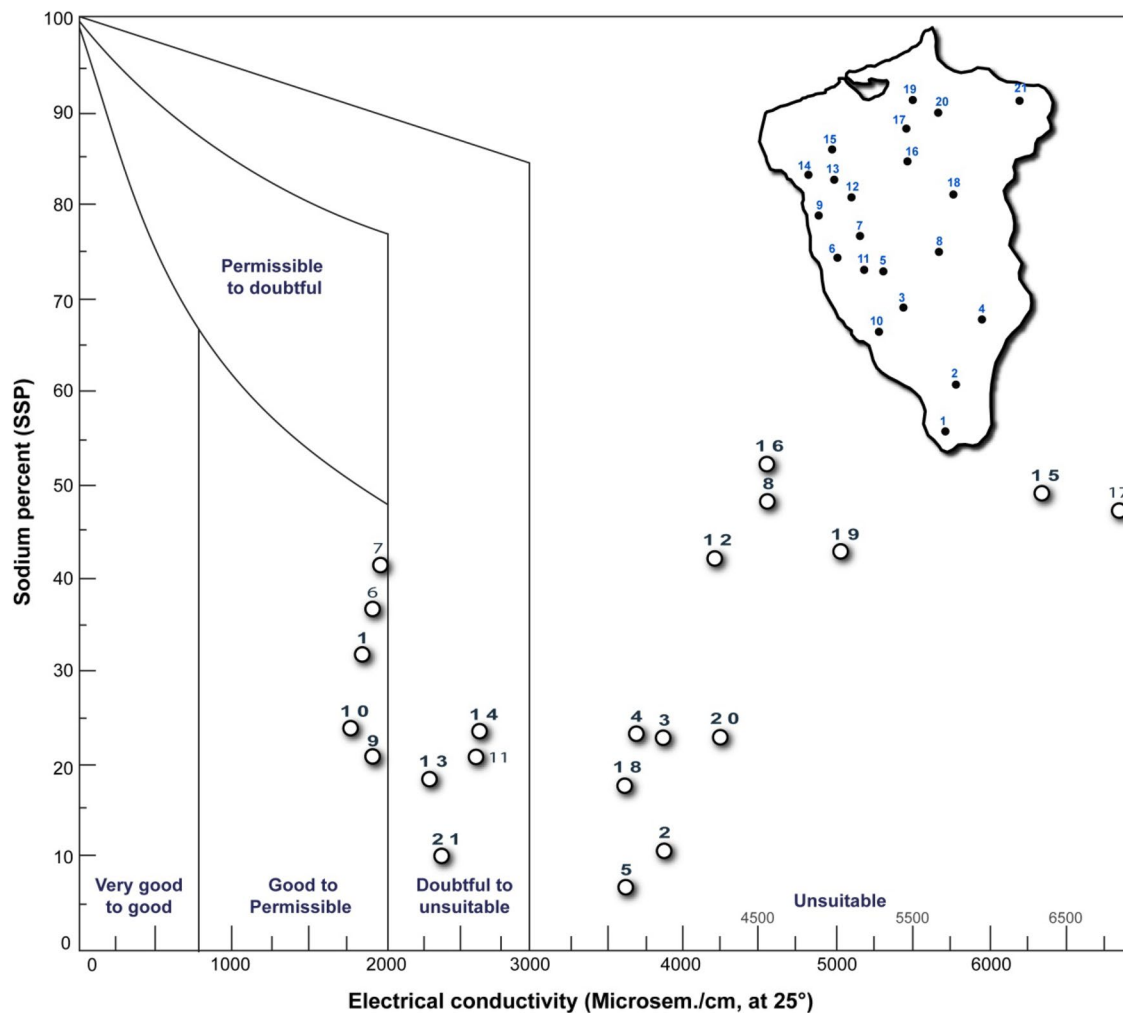


**Fig. 8** Wilcox diagram for suitability of water for irrigation

chemical composition of groundwater in this area is dominated by the ions  $\text{Cl}^-$ ,  $\text{SO}_4^{2-}$ ,  $\text{Na}^+$  and  $\text{Ca}^{2+}$ . The strongly acidic chloride and sulfate ions were found to dominate the anionic composition of groundwater and sodium is the dominant cation. These ions may have the same origin, possibly related to dissolution of halite.

The major ions are classified into four categories based on a scatter matrix analysis.  $\text{Na}^+$  shows a high level of ionic interdependence and hydrochemical interaction. Concentrations of several ions exhibit good linear correlations with  $\text{Cl}^-$  which is also confirmed by TDS diagram analysis. The Na–Cl dissolution process seems to be dominant in the GB aquifer. Moreover, the groundwater mineralization and chemistry are mainly controlled by reverse ion exchange.

The suitability of groundwater for irrigation use was also assessed using a geospatial mapping approach of a hydrochemical data combined with classifications from USSL and Wilcox diagrams. In general at the GB scale,

the western margin of the pediplain seems to be the most suitable area for adequate and safe irrigation with a groundwater potential estimated to 24%. Most water samples were considered to be either unsuitable or moderately suitable for irrigation use, particularly in the northern part of the study area where highly saline soils associated with a sebkha seem affecting the groundwater quality. Anthropogenic activities and sodium enrichment are jointly causing water quality deterioration in the GB aquifer. However, it is possible to improve the quality of water samples deemed unfavorable for irrigation by applying adequate treatments. This strategy will be mandatory especially in this region where agricultural is a main activity.

**Acknowledgements** The authors are grateful to Dr. Gunter Dörhöfer, Editor-in-Chief of the *Journal of Environmental Earth Sciences*, the associate editor who handled this manuscript and the anonymous reviewers for their constructive review and useful comments on the manuscript.



## References

- Abu-alnaeem MF, Yusoff I, Fatt Ng T, Alias Y, Raksmei M (2018) Assessment of groundwater salinity and quality in Gaza coastal aquifer, Gaza Strip, Palestine: an integrated statistical, geostatistical and hydrogeochemical approaches study. *Sci Total Environ* 615:972–989
- Alam M, Rais S, Aslam M (2012) Hydrochemical investigation and quality assessment of ground water in rural areas of Delhi, India. *Environ Earth Sci* 66:97–110. <https://doi.org/10.1007/s12665-011-1210-x>
- Ameur M, Hamzaoui-Azaza F, Gueddari M (2016) Suitability for human consumption and agriculture purposes of Sminja aquifer groundwater in Zaghuan (north-east of Tunisia) using GIS and geochemistry techniques. *Environ Geochem Health* 38:1147–1167. <https://doi.org/10.1007/s10653-015-9780-2>
- Andersen CB (2001) The problem of sample contamination in a fluvial geochemistry research experience for undergraduates. *J Geosci Educ* 49:351–357
- APHA (1998) Standard methods for the examination of water and wastewater, vol 20. American Public Health Association (APHA), Washington, DC
- Argamasilla M, Barberà JA, Andreo B (2017) Factors controlling groundwater salinization and hydrogeochemical processes in coastal aquifers from southern Spain. *Sci Total Environ* 580(February 2017):50–68 15
- Arnould M (1950) Carte géologique de la Tunisie au 1/50 000, Feuille N°22 Menzel Bouzelfa. Office National des Mines, Tunisie
- Arnould P, Hotyat M (2003) Eau et environnement. Tunisie et milieux méditerranéens. ENS, Lyon
- Arslan H (2013) Application of multivariate statistical techniques in the assessment of groundwater quality in seawater intrusion area in Bafra Plain. *Turkey Environ Monit Assess* 185:2439. <https://doi.org/10.1007/s10661-012-2722-x>
- Bedir M, Tlig S, Bobier C, Aissaoui N (1996) Sequence stratigraphy, basin dynamics, and petroleum geology of the Miocene from eastern Tunisia. *AAPG Bull* 80(1):63–80
- Ben Ayed N (1993) Evolution tectonique de l'avant-pays de la chaîne alpine de Tunisie du début du Mésozoïque à l'Actuel. *Ann Mines Geol Ed Serv Géol Tunisie* 32:1–286
- Ben Ismail-Latrache K, Bobier C (1984) Sur l'évolution des paléoenvironnements marins paléogènes des bordures occidentales du détroit Siculo-Tunisien et leurs rapports avec les fluctuations du paléo-océan mondial. *Mar Geol* 55:195–217
- Ben Moussa A, Zouari K, Oueslati N (2009) Geochemical study of groundwater mineralization in the Grombalia shallow aquifer, north-eastern Tunisia: implication of irrigation and industrial waste water accounting. *Environ Geol* 58:555–566. <https://doi.org/10.1007/s00254-008-1530-7>
- Ben Salem H (1992) Contribution à la connaissance de la géologie du Cap Bon: Stratigraphie, Tectonique et Sédimentologie. Dissertation, Faculté des Sciences de Tunis, University of Tunis El Manar
- Bennetts DA, Webb JA, Stoneb DJM, Hill DM (2006) Understanding the salinisation process for groundwater in an area of south-eastern Australia, using hydrochemical and isotopic evidence. *J Hydrol* 323(1–4):178–192. <https://doi.org/10.1016/j.jhydrol.2005.08.023>
- Biely A, Rakús M, Robinson P, Salaj J (1972) Essai de corrélation des formations miocènes au sud de la Dorsale tunisienne. *Not Serv Géol Tunisie* 38:73–93
- Boughariou E, Bahloul M, Jmal I, Allouche N, Makni J, Khanfir H, et Bouri S (2018) Hydrochemical and statistical studies of the groundwater salinization combined with MODPATH numerical model: case of the Sfax coastal aquifer, Southeast Tunisia. *Arab J Geosci* 11:69. <https://doi.org/10.1007/s12517-018-3408-7>
- Bouksila F, Bahri A, Berndtsson R, Persson R, Rozema J, Van der Zee S (2013) Assessment of soil salinization risks under irrigation with brackish water in semiarid Tunisia. *Environ Exp Bot* 92:176–185. <https://doi.org/10.1016/j.envexpbot.2012.06.002>
- Bujalka P, Johan Z, Krivy M, Rakus M, Vacek J (1971) Carte géologique de la Tunisie, Grombalia à l'échelle 1/50000. Notes du service Géologique de Tunisie
- Burollet PF (1956) Signification géologique de l'axe Nord-Sud. Actes du 1er Congrès Nat Sci Terre, Tunisie, pp 315–319
- Carol E, Kruse E, Mas-Pla J (2009) Hydrochemical and isotopic evidence of ground water salinization processes on the coastal plain of Samborombón Bay, Argentina. *J Hydrol* 365:335–345
- Castany G (1948) Les fossés d'effondrement de Tunisie, Géologie et Hydrologie. Plaine de Grombalia et cuvettes de la Tunisie Orientale. Premier fascicule. *Ann Mines Géol* (3), ONM, Tunis
- Chakroun A, Zaghbib-Turki D, Miskovsky JC, Davaud E (2009) Two Tyrrhenian transgressive cycles in coastal deposits of the Cap Bon Peninsula, Tunisia. *Quaternaire* 20:215–226. <https://doi.org/10.4000/quaternaire.5140>
- Chen C-H, Wang C-H, Wen S, Yeh T-K, Lin C-H., Liu J-Y, Yen H-Y, Lin C, Rau R-J, Lin T-W (2013) Anomalous frequency characteristics of groundwater level before major earthquakes in Taiwan. *Hydrol Earth Syst Sci* 17:1693–1703
- Chihi L (1995) Les fossés néogènes quaternaires de la Tunisie et de la mer Pélagienne: une étude structurale et une signification dans le cadre géodynamique de la Méditerranée centrale. Dissertation, University of Tunis II
- Custodio E (1993) Coastal aquifer salinization as a consequence of aridity: the case of Amurga phonolitic massif, Gran Canaria Island. In: Study and modelling of saltwater intrusion. CIMNE-UPC, Barcelona, pp 81–98
- Danielsson A, Cato I, Carman R, Rahm L (1999) Spatial clustering of metals in the sediments of the Skagerrak/Kattegat. *Appl Geochem* 14:689–706
- Davis JC (2002) Statistics and data analysis in geology, 3rd ed. Wiley, Oxford
- DGRE Direction Générale des Ressources en Eaux (1998) Réseau de suivi de la qualité des eaux souterraines en Tunisie. Report, Tunis
- Dhraief W, Dhahri F, Chalwati I, Boukadi N (2017) Tectonostratigraphic framework of Upper Cretaceous—Neogene series in the Gulf of Tunis inferred from subsurface data: implications for petroleum exploration. *Geol Carpath* 68(2):97–108. <https://doi.org/10.1515/geoca-2017-0008>
- Elango L, Suresh Kumar S, Rajmohan N (2003) Hydrochemical studies of groundwater in Chengalpet region, South India. *Indian J Environ Prot* 23(6):624–632
- Ennabli M (1980) Etude hydrogéologique des aquifères du Nord-Est de la Tunisie pour une gestion intégrée des ressources en eau. Thesis, Nice University, France
- Freeze RA, Cherry JA (1979) Groundwater. Prentice-Hall, Englewood Cliffs (ISBN:978-0133653120)
- Gil-Márquez JM, Barberá JA, Andreo B, Mudarra M (2017) Hydrological and geochemical processes constraining groundwater salinity in wetland areas related to evaporitic (karst) systems. A case study from Southern Spain. *J Hydrol* 544:358–554
- Gupta S, Nayek S, Chakraborty D (2016) Hydrochemical evaluation of Rangit river, Sikkim, India: using Water Quality Index and multivariate statistics. *Environ Earth Sci* 75:567. <https://doi.org/10.1007/s12665-015-5223-8>
- Hadji Sassi M, Zouari H, Jallouli C (2006) Gravity and seismic contribution for a new geodynamic interpretation of troughs in Tunisia: the example of the Grombalia trough. *Comptes Rendus Geosci* 338:751–756. <https://doi.org/10.1016/j.ctre.2006.07.005>
- Hiscock KM (2005) Hydrogeology: principles and practice. Wiley, New York, p 389 (ISBN: 978019857634)

- Kelly WP (1951) Alkali soils—their formation properties and reclamation, 3rd edn. Reinhold Publication, New York, p 92
- Khaki M, Yusoff I, Ismalami N (2015) Application of the artificial neural network and neurofuzzy system for assessment of groundwater quality. *Clean Soil Air Water* 43(4):551–560
- Kim MJ, Nriagu J, Haack S (2002) Arsenic species and chemistry in groundwater of southeast Michigan. *Environ Pollut* 120:379–390
- Kim G, Lee KK, Park KS, Hwang DW, Yang HS (2003) Large submarine groundwater discharge (SGD) from a volcanic island. *Geophys Res Lett* 30:21
- Liu W, Wei X, Li Q, Fan H, Duan H, Wu J, Giles-Hansen K, Zhang H (2016) Hydrological recovery in two large forested watersheds of southeastern China: the importance of watershed properties in determining hydrological responses to reforestation. *Hydrol Earth Syst Sci* 20:4747–4756
- Melki F, Zouaghi T, Ben Chelbi M, Bédir M, Zargouni F (2010) Tectono-sedimentary events and geodynamic evolution of the Mesozoic and Cenozoic basins of the Alpine Margin, Gulf of Tunis, north-eastern Tunisia offshore. *CR Geosci* 342:741–753
- Mohapatra PK, Vijay R, Pujari PR, Sundaray SK, Mohanty BP (2011) Determination of processes affecting groundwater quality in the coastal aquifer beneath Puri city, India: a multivariate statistical approach. *Water Sci Technol* 64(4):809–817
- Mor S, Ravindra K, Dahiya RP, Chandra A (2006) Leachate characterization and assessment of groundwater pollution near municipal solid waste landfill site. *Environ Monit Assess* 118:435–456. <https://doi.org/10.1007/s10661-006-1505-7>
- Mosaferi M, Pourabbar M, Shakerkhatibi M, Fatehifar E, Belyasi M (2014) Quality modeling of drinking groundwater using GIS in rural communities, northwest of Iran. *J Environ Health Sci Eng* 12:99
- Ntanganedzeni B, Elumalai V, Rajmohan N (2018) Coastal aquifer contamination and geochemical processes evaluation in Tugela catchment, South Africa geochemical and statistical approaches. *Water* 10(6):687. <https://doi.org/10.3390/w10060687>
- Okiongbo KS, Douglas R (2015) Evaluation of major factors influencing the geochemistry of groundwater using graphical and multivariate statistical methods in Yenagoa city, Southern Nigeria. *Appl Water Sci* 5:27
- Origin Pro (2015) Origin user guide, OriginLab ed. Northampton, MA, p 285
- Papatheodorou G, Lambrakis N, Panagopoulos G (2007) Application of multivariate statistical procedures to the hydrochemical study of a coastal aquifer: an example from Crete, Greece. *Hydrogeol Process* 21(11):1482–1495
- Petalas C, Lambrakis N (2006) Simulation of intense salinization phenomena in coastal aquifers—the case of the coastal aquifers of Thrace. *J Hydrol* 324(1–4):51–64
- Raghunath HM (1987) Groundwater. Wiley Eastern Ltd., New Delhi
- Richards LA (1954) Diagnosis and improvement of saline and alkali soils. In: *Agricultural handbook* 60. USDA, Washington DC, p 160
- Rusydi FA (2018) Correlation between conductivity and total dissolved solid in various type of water: a review. *IOP Conf Ser Earth Environ Sci* 118:012019. <https://doi.org/10.1088/1755-1315/118/1/012019>
- Salem ZE, Atwia MG, El-Horiny MM (2015) Hydrogeochemical analysis and evaluation of groundwater in the reclaimed small basin of Abu Mina, Egypt. *Hydrogeol J* 23:1781–1797. <https://doi.org/10.1007/s10040-015-1303-9>
- Sebei A, Chaabani F, Souissi F, Abdeljaoued S (2004) Hydrologie et qualité des eaux de la nappe de Grombalia (Tunisie nord-orientale). *Sécheresse* 15:159–166
- Smith BK, Smith JA, Baeck ML, Miller AJ (2015) Exploring storage and runoff generation processes for urban flooding through a physically based watershed model. *Water Resour Res* 51(3):1552–1569
- Taylor EW (1958) The examination of water and water supplies. Church Hill Ltd., UK
- Thivya C, Chidambaram S, Rao MS, Thilagavathi MV, Manikanda S (2017) Assessment of fluoride contaminations in groundwater of hard rock aquifers in Madurai district, Tamil Nadu (India). *Appl Water Sci* 7:1011. <https://doi.org/10.1007/s13201-015-0312>
- Tlili-Zrelli B, Hamzaoui-Azaza F, Gueddari M, Bouhlila R (2013) Geochemistry and quality assessment of groundwater using graphical and multivariate statistical methods. A case study: Grombalia phreatic aquifer (Northeastern Tunisia). *Arabian J Geosci* 6(9):3545–3561
- Trabelsi F, Tarhouni J, Ben Mammou A, Ranieri G (2013) GIS-based subsurface databases and 3-D geological modeling as a tool for the set up of hydrogeological framework: Nabeul-Hammamet coastal aquifer case study (Northeast Tunisia). *Environ Earth Sci* 70:2087–2105. <https://doi.org/10.1007/s12665-011-1416-y>
- Tziritis E, Skordas K, Kelepertsis A (2016) The use of hydrogeochemical analyses and multivariate statistics for the characterization of groundwater resources in a complex aquifer system. A case study in Amyros River basin, Thessaly, central Greece. *Environ Earth Sci* 75:339. <https://doi.org/10.1007/s12665-015-5204-y>
- Wang Y, Jiao JJ (2012) Origin of groundwater salinity and hydrogeochemical processes in the confined Quaternary aquifer of the Pearl River Delta China. *J Hydrol* 438–439:112–124. <https://doi.org/10.1016/j.jhydrol.2012.03.008>
- WHO (2011) Guidelines for drinking-water quality, V.1. Recommendations. World Health Organization, Geneva (ISBN: 9789241548151)
- Wilcox LV (1995) Classification and use of irrigation water. US Department of Agriculture. Washington Dc, p 19